PHYSICAL REVIEW B **94**, 205109 (2016)

Quasi-one-dimensional spin-orbit-coupled correlated insulator in a multinuclear coordinated organometallic crystal

J. Merino
Departamento de Física Teórica de la Materia Condensada, Condensed Matter Physics Center (IFIMAC) and Instituto Nicolás Cabrera, Universidad Autónoma de Madrid, Madrid 28049, Spain

A. C. Jacko, A. L. Khosla, and B. J. Powell
School of Mathematics and Physics, The University of Queensland, Brisbane, Queensland 4072, Australia
(Received 24 June 2016; revised manuscript received 26 September 2016; published 4 November 2016)

We show how quasi-one-dimensional correlated insulating states arise at two-thirds filling in organometallic multinuclear coordination complexes described by layered decorated honeycomb lattices. The interplay of spin-orbit coupling and electronic correlations leads to pseudospin-one moments arranged in weakly coupled chains with highly anisotropic exchange and a large trigonal splitting. We show that the in-plane exchange coupling is very different from the interlayer coupling; in particular the latter is much larger, despite the underlying hopping integrals being close to isotropic. Surprisingly, the effective dimensionality of the pseudospin model is strongly dependent on the strength of the electronic correlations: With increasing Hubbard U the pseudospin-one model becomes increasingly one dimensional, even though the crystal is almost isotropic. We predict that the trigonal splitting leads to a quantum phase transition from a Haldane phase to a topologically trivial phase as the relative strength of the spin-orbit coupling increases.

DOI: 10.1103/PhysRevB.94.205109

I. INTRODUCTION

In recent years there has been intense research activity on the effect of spin-orbit coupling (SOC) in the electronic structure of weakly interacting materials since the discovery of topological band insulators [1,2]. Topological band insulators are predicted to occur in certain solids with electronlike quasiparticles in the presence of strong SOC as is found in compounds containing the heavy elements such as: Bi, Pb, Sb, Hg, and Te. In materials with partially filled localized orbitals, renormalization effects induced by strong Coulomb repulsion effectively enhance the SOC leading, for instance, to topological Mott [3,4] or Kondo [5] insulators. In Ir-based compounds such as Na_2IrO_3 and Li_2IrO_3 the emergent $J = 1/2$ pseudospins arranged in a honeycomb lattice interact through anisotropic spin exchange couplings of the Kitaev-Heisenberg type [6–9]. Kitaev's honeycomb model can be solved exactly [10] sustaining a topological quantum spin liquid state with Majorana fermion excitations which may have been recently observed in the Kitaev candidate material [11] α-$RuCl_3$. This illustrates how quantum phases of matter arise from the interplay of strong Coulomb repulsion and SOC in certain materials.

Molecular materials are ideal playgrounds to explore strong electronic correlation effects in low dimensions [12,13]. Although SOC effects are generally weak in organic systems [14], organometallic complexes provide a route for enhancing SOC [15]. Llusar *et al.* have synthesized a particularly interesting family of trinuclear organometallic coordination complexes [16,17] with ligands that facilitate electronic transport between molecules including $Mo_3S_7(dmit)_3$, $Mo_3Se_7(dmit)_3$, $Mo_3S_7(dsit)_3$, and $Mo_3Se_7(dsit)_3$ (dmit = S_5C_3, dsit = $Se_2S_3C_3$). For example, the low-energy electronic structure of $Mo_3S_7(dmit)_3$ crystals [18] is described by three Wannier orbitals per molecule that are hybrids of the Mo d orbitals and the dmit molecular orbitals leading to narrow band structures with appreciable SOC [19,20]. The Mo atoms, and hence the Wannier orbitals, form a layered structure with a decorated honeycomb lattice in the basal plane [19], as shown in Fig. 1. In the c direction, the triangular $Mo_3S_7(dmit)_3$ complexes arrange in tubes reminiscent of the CrAs tubes formed in the recently discovered superconductor $K_2Cr_3As_3$ [21,22].

It has recently been shown that, in the absence of SOC, Hubbard models on lattices of triangles coupled in one dimension are insulators at two-thirds filling. Similar results are found for both the triangular necklace lattice [23,24], where the triangles are coupled through a single vertex, and the three legged ladder lattice [25], where all three vertices of the triangle are coupled to the corresponding vertex in nearest neighboring triangles. In both models the insulating phase is characterized by effective spin-one moments on the triangle that are coupled through an isotropic antiferromagnetic interaction [23–25]. Remarkably, at two-thirds filling, this phase arises even in the pure Hubbard model with no off-site Coulomb interactions.

In this paper, we derive the effective superexchange model, including the effects of SOC, for crystals of trinuclear complexes. SOC entangles the spin and orbital degrees of freedom leading to pseudospin-one moments $\boldsymbol{\mathcal{S}}_m$ on the mth triangle, which interact via anisotropic exchange interactions. The SOC also introduces a trigonal splitting of the triplet into a lower energy $\mathcal{S}^z_m = 0$ state and a $\mathcal{S}^z_m = \pm 1$ doubly degenerate state. Surprisingly, we also find that the effective dimensionality of the pseudospin model is strongly affected by the strength of the electronic correlations: With increasing Hubbard U the pseudospin-one model becomes increasingly one dimensional, even though the original crystal is almost isotropic. At large trigonal splitting, a 'D phase,' consisting of the tensor product of $\mathcal{S}^z_m = 0$ states on each complex, occurs. Thus, our analysis suggests that a topological quantum phase transition from a Haldane phase to a topologically trivial D phase can be induced by increasing the SOC.

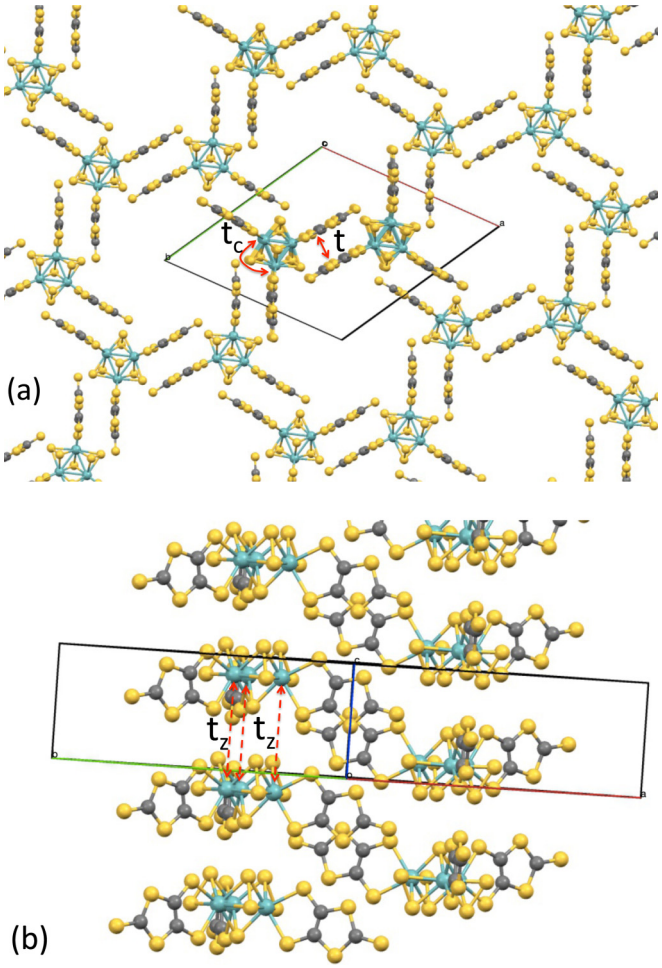

FIG. 1. Crystal structure of $Mo_3S_7(dmit)_3$. In the a-b plane the triangular molecules form a honeycomb lattice. As each complex contains three Wannier orbitals this results in a decorated lattice (a), which extrapolates between the kagome and graphene lattices [19]. Complexes stack in chains along the c axis resulting in a triangular tube arrangement (b) of the Wannier orbitals. The hopping amplitudes: t_c, t, and t_z entering model (1) are explicitly shown for clarity and tabulated in Table I.

II. PSEUDOSPIN-ONE MOMENTS IN TRINUCLEAR COMPLEXES

We first analyze the local effective spin degrees of freedom arising at each isolated trimer due to the combined effect of Coulomb repulsion and SOC. We construct our model based on the Wannier orbitals found in recent density functional calculations [19,20], and we model each complex via a Hubbard-Heisenberg model on a triangle with one orbital per site. The precise form of the SOC contribution in both even and odd cyclic molecules has been previously derived based on general symmetry arguments [20]. In molecules with cyclic symmetry, such as the C_3 symmetry of a $Mo_3S_7(dmit)_3$ complex, the leading SOC term in the effective low-energy Hamiltonian couples the electron spin to currents running around the complex [20], which carry a 'molecular' orbital angular momentum $\boldsymbol{L}_m$. For molecules with N-fold rotation axes the angular momentum carried by this current is $l = (N-1)/2$ if N is odd [20]; for a $Mo_3S_7(dmit)_3$ complex $N = 3$ and $l = 1$. Thus the Hamiltonian for the mth complex is $H_c = H_0 + H_{\rm int} + H_{\rm SO}$, where

$$H_0 = -t_c \sum_{\langle ij\rangle\sigma} (c^\dagger_{mi\sigma} c_{mj\sigma} + \text{H.c.})$$

$$H_{\rm int} = U \sum_i n_{mi\uparrow} n_{mi\downarrow} + J_F \sum_{\langle ij\rangle} \left(\mathbf{S}_{mi} \cdot \mathbf{S}_{mj} - \frac{n_{mi} n_{mj}}{4} \right)$$

$$H_{\rm SO} = \lambda_{xy} \left(L^x_m S^x_m + L^y_m S^y_m \right) + \lambda_z L^z_m S^z_m, \quad (1)$$

$c^{(\dagger)}_{mi\sigma}$ annihilates (creates) an electron with spin σ in the ith Wannier orbital of the mth molecule, $\mathbf{S}_{mi} = \sum_{\sigma\sigma'} c^\dagger_{mi\sigma} \boldsymbol{\tau}_{\sigma\sigma'} c_{mi\sigma'}$ is the electronic spin operator, $\boldsymbol{\tau}$ is the vector of Pauli matrices, $\mathbf{S}_m = \sum_i \mathbf{S}_{mi}$, $n_{mi\sigma} = c^\dagger_{mi\sigma} c_{mi\sigma}$, and $n_{mi} = \sum_\sigma n_{mi\sigma}$, t_c is the intramolecular hopping amplitude, U is the onsite Coulomb repulsion, and $J_F < 0$ is the direct intramolecular ferromagnetic exchange [26]. We take the z direction along the c direction of the crystal. We consider the three-site cluster with four electrons, relevant to $Mo_3S_7(dmit)_3$ and its selenated analogs. In Table I we list the parameters obtained from *ab initio* methods [19] for the model (1).

TABLE I. Values of the one-electron parameters of the models discussed here for $Mo_3S_7(dmit)_3$ as derived from density functional calculations in Refs. [19,20]. The strength of the interactions (U, J_F) are not well known. One expects that the SOC will be significantly enhanced (by up to an order of magnitude) in the selenated analogues of $Mo_3S_7(dmit)_3$; however, these have not been calculated to date.

Parameter	(meV)	Description	Ref.
t_c	59.69	intramolecular hopping	[19]
λ_{xy}	3.54	parallel molecular SOC	[20]
λ_z	4.91	perpendicular molecular SOC	[20]
t	47.11	in-plane hopping	[19]
t_z	40.85	inter-plane hopping	[19]

The single electron terms are more conveniently expressed in terms of 'Bloch' operators on the trimer,

$$b^\dagger_{mk\sigma} = \frac{1}{\sqrt{3}} \sum_j c^\dagger_{mj\sigma} e^{i\phi kj}, \quad (2)$$

where $\phi = 2\pi/3$ and $k = 0, \pm 1$ is the eigenvalue of L^z_m [15,20,27]. Whence,

$$H_0 = -2t_c \sum_{k\sigma} \cos(k\phi) b^\dagger_{mk\sigma} b_{mk\sigma}$$

$$H_{\rm SO} = \frac{\lambda_{xy}}{\sqrt{2}} (b^\dagger_{m0\downarrow} b_{m-1\uparrow} - b^\dagger_{m1\downarrow} b_{m0\uparrow} - b^\dagger_{m0\uparrow} b_{m1\downarrow} + b^\dagger_{m-1\uparrow} b_{m0\downarrow}) + \frac{\lambda_z}{2} (b^\dagger_{m1\uparrow} b_{m1\uparrow} - b^\dagger_{m1\downarrow} b_{m1\downarrow} - b^\dagger_{m-1\uparrow} b_{m-1\uparrow} + b^\dagger_{m-1\downarrow} b_{m-1\downarrow}). \quad (3)$$

Note that the trigonal symmetry of the complex implies that the SOC in the plane of the molecule, λ_{xy}, need not equal that in the z direction [20]. Nevertheless, in some of the numerical work below it is convenient to set $\lambda = \lambda_{xy} = \lambda_z$ to reduce the parameter space.

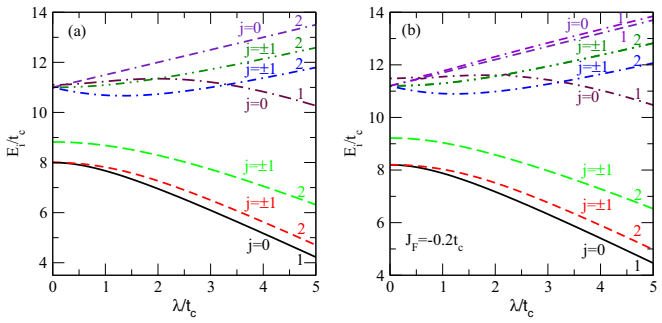

FIG. 2. Effective pseudospin-one moments arising in isolated trimers in the presence of SOC. The lowest-lying eigenstates of the Hubbard-Heisenberg model describing trinuclear complexes with four electrons are shown for the pure Hubbard model ($U = 10t_c, J_F = 0$) (a) and for nonzero intracluster exchange (b) ($U = 10t_c, J_F = -0.2t_c$). Only the z component of the total angular momentum j is conserved. The degeneracies of the eigenstates are labeled by the numbers on the right-hand side of the figure. As SOC, $\lambda = \lambda_{xy} = \lambda_z$, increases the triplet state is split into a $j = 0$ state and a doubly degenerate $j = \pm 1$ state. This is described by a pseudospin-one in the presence of a trigonal field generated by SOC.

Spin-orbit coupling can only mix configurations with the same z component of the total orbital momentum of the cluster: j, which is conserved (modulo 3) for any values of λ_{xy},λ_z. With no SOC and $t_c > 0$ the low lying states are the triplet states [28], even at $J_F = 0$. In Fig. 2 we show how the cluster spectrum for $\lambda \neq 0$ consists of a $|j = 0\rangle$ ground state and doubly degenerate $|j = \pm 1\rangle$ states, expected from the combination of time reversal and trigonal (C_3) symmetries. At large U the three lowest states behave as a localized pseudospin-one. In terms of the pseudospins the effective low energy Hamiltonian for a single complex is thus $H_c^{\rm eff} = D(\mathcal{S}_m^z)^2$; D is the trigonal splitting which increases with λ, cf. Figs. 2 and 4.

III. EXCHANGE INTERACTION BETWEEN NEIGHBORING TRINUCLEAR COMPLEXES

We now consider the interaction between two neighboring trimers arranged as in the $Mo_3S_7(dmit)_3$ crystal. We analyze the two nearest-neighbor arrangements realized in the crystal.

(A) Nearest neighbors in the a-b plane [Fig. 1(a)]: a single hopping amplitude t connects the two molecules:

$$H_{\rm kin} = -t \sum_{\sigma} (c^{\dagger}_{l1\sigma} c_{m1\sigma} + c^{\dagger}_{m1\sigma} c_{l1\sigma}) \tag{4}$$

[cf. inset Fig. 4(a)]. We will refer to this as the dumbbell configuration.

(B) Nearest neighbors in the c direction [Fig. 1(b)]: There are three hoppings, t_z, connecting equivalent orbitals i of the two molecules:

$$H_{\rm kin} = -t_z \sum_{i\sigma} (c^{\dagger}_{li\sigma} c_{mi\sigma} + c^{\dagger}_{mi\sigma} c_{li\sigma}) \tag{5}$$

[cf. inset Fig. 4(d)]. Thus the complexes form three legged ladders (i.e., tubes) along the c axis.

From $Mo_3S_7(dmit)_3$ first principles calculations (see Table I) it is found that the intermolecular hopping is almost isotropic: $t_z/t = 0.87$.

Some understanding of these models can be gained from previous studies of the Hubbard model [which is the $J_F = \lambda = 0$ limit of the current model, Eq. (1)] on the necklace lattice [23,24] and on the three legged ladder [25]. The former is the one-dimensional analog of arrangement (A), whereas the latter is the extended lattice realization of (B). In both models, a Haldane insulator with a charge gap and a small spin gap is found down to small values of U. This is in contrast with naive expectations since with four electrons per trimer, the system is away from half filling and so is expected to be metallic. In the triangular necklace lattice a 'local parity' symmetry protects the insulating phase from strong charge fluctuations developing as U decreases [23,24]. However, this symmetry is absent in the three legged ladder and significantly larger charge fluctuations are observed in this model [25]. Nevertheless for large U and two-thirds filling (an average of four electrons per triangle) both lattices have insulating phases with effective spin-one moments. Motivated by this previous analysis and the results of Sec. II we now derive an effective spin exchange model for the insulator in the presence of SOC, which is justified in the large-U limit.

We have calculated the effective exchange coupling between two neighboring clusters via two independent methods: (1) analytically via a canonical transformation to first order in $1/U$ and second order in $H_{\rm SO}$ and $H_{\rm kin}$ and (2) numerically with H_c treated exactly and straightforward second order perturbation theory in $H_{\rm kin}$:

$$H^{(2)}_{\rm eff} = \sum_{|m_0\rangle} \frac{H_{\rm kin}|m_0\rangle\langle m_0|H_{\rm kin}}{2E_0(4) - \langle m_0|H_0 + H_U + H_{\rm SOC}|m_0\rangle}, \tag{6}$$

where $\{|m_0\rangle\}$ is the complete set of virtual states with three electrons in one trimer and five electrons in the other. $E_0(4)$ is the ground state energy of an isolated cluster with $N = 4$ electrons.

The reliability of the second order perturbation expansion can be tested by comparison of the spectrum obtained from diagonalizing $H^{(2)}_{\rm eff}$ with the exact eigenspectrum of two coupled trimers as shown in Fig. 3 for $U = 10t_c$. Second order perturbation theory in $H_{\rm kin}$ is found to be extremely accurate in the dumbbell arrangement for any λ. In the tube arrangement it is more accurate for $\lambda > t_c/2$ than for smaller λ. However, we have checked that with increasing U the perturbative eigenspectrum converges to the exact solution for any λ indicating the reliability of the perturbative treatment at sufficiently large U. The route we take is as follows. We use the canonical transformation to obtain analytically the relevant spin-spin interactions entering the low energy effective Hamiltonian at strong coupling. By identifying these interactions with the ones obtained from second order perturbation theory we extract numerical values of the corresponding matrix elements which are exact to all orders in λ.

A simple measure of the errors due to neglecting matrix elements that only appear beyond second order in λ is to calculate the largest eigenvalue of the residual of the full set of matrix elements minus the effective Hamiltonian. We have

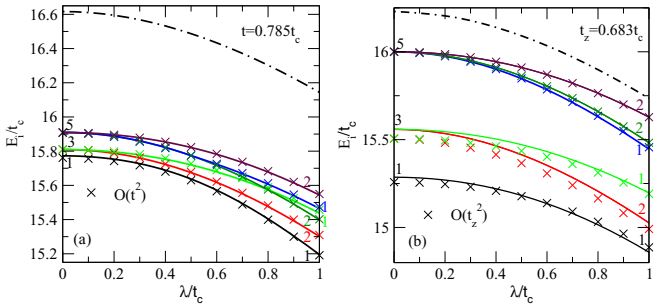

FIG. 3. Comparison of the exact eigenspectrum (lines) of two coupled triangular clusters with the eigenspectrum obtained from the second order perturbation theory effective model (crosses), $H^{(2)}_{\rm eff}$. In (a) we show the case of two trimers coupled in the dumbbell arrangement through the hopping $t = 0.785t_c$, while (b) corresponds to two trimers coupled in the tube arrangement through $t_z = 0.683t_c$. In both cases we take $U = 10t_c$. The black dot-dashed curves represent the lowest energy eigenstate of the exact solution that is not included in the effective spin model.

done this at all parameters discussed and find this residual to be small throughout, see below.

A. Nearest neighbors in the *a*-*b* plane

Two neighboring molecules, l and m, related by inversion symmetry satisfy: $\lambda_{m,xy} = \lambda_{l,xy}$ and $\lambda_{m,z} = \lambda_{l,z}$. The canonical transformation yields an effective pseudospin model consisting of onsite and nearest neighbor terms:

$$H^{\rm eff}_{ab} = \sum_{\langle lm\rangle\alpha\beta} J^{ab}_{\alpha\beta}\mathcal{S}^{\alpha}_{l}\mathcal{S}^{\alpha}_{m} + \sum_{l}\Big\{D\big(\mathcal{S}^{z}_{l}\big)^2 + \big[K_{\pm\pm}\mathcal{S}^{+}_{l}\mathcal{S}^{+}_{l} + \eta K_{z\pm}\mathcal{S}^{z}_{l}\mathcal{S}^{x}_{l} + \text{H.c.}\big]\Big\}, \qquad (7)$$

with $\eta = 1$, $J^{ab}_{\alpha\beta} = J^{ab}_{\beta\alpha}$, $\alpha,\beta = x,y,z$ and angled brackets imply that the sum is over nearest neighbors only avoiding double counting. The model parameters obtained from the canonical transformation are given in Appendix A. The matrix elements calculated from the numerical perturbation theory are in excellent agreement with this model, even for $\lambda > t_c$. This is not entirely surprising because λ/U remains small in this limit. The small residual terms (see Appendix) have the symmetry one would expect on extrapolating Eq. (7) to higher orders in $H_{\rm SO}$ [29].

In the pure Hubbard model ($J_F = 0$) we find numerically that there are no additional terms at higher order in $1/U$ or λ, furthermore the exchange coupling tensor is diagonal, $J^{ab}_{\alpha\beta} = J^{ab}_{\alpha\alpha}\delta_{\alpha\beta}$, and $K_{z\pm} = K_{\pm\pm} = 0$. We plot the dependence of D and $J^{ab}_{\alpha\alpha}$ on λ for fixed $U = 10t_c$ in Fig. 4(a). The exchange couplings only display a very weak anisotropy, $J^{ab}_{xx} = J^{ab}_{yy} \approx J^{ab}_{zz}$, indicating that the coupling can be described through a standard isotropic Heisenberg model in the presence of a trigonal splitting induced by SOC. Note that the trigonal splitting D increases with increasing λ, and around $\lambda \approx 0.5t_c$ it becomes comparable to the exchange: $D \approx J^{ab}_{\alpha\alpha}$. At large values of $D \gtrsim J^{ab}_{\alpha\alpha}$, a large-$D$ phase simply given by the tensor product of $j = 0$ states located on each cluster is expected. For instance, in the one-dimensional $S = 1$ chain a quantum phase transition from the Haldane phase to the large-D phase occurs [30–33] for $D/J \sim 0.96$–0.971.

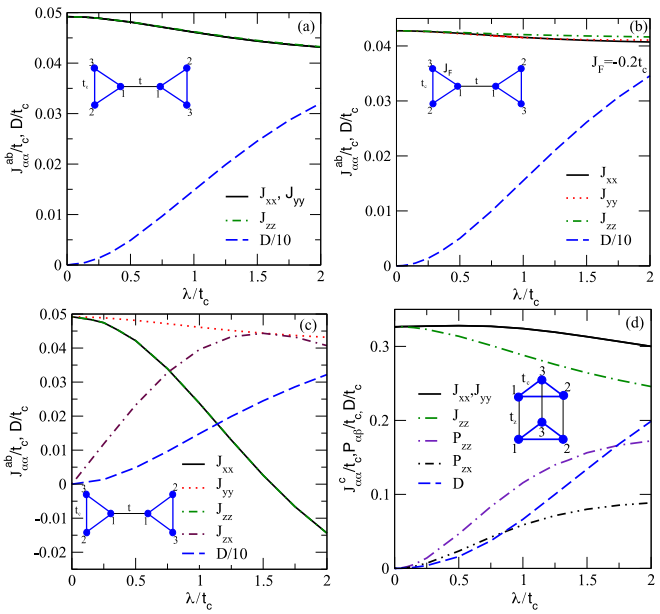

FIG. 4. Anisotropic pseudospin exchange coupling $J^{\nu}_{\alpha\beta}$ and trigonal splitting D induced by spin-orbit coupling in trinuclear complexes. Here $\nu = ab$ labels the exchange interaction in the basal plane (dumbbell model), while $\nu = c$ indicates the exchange interactions along the chains (tube model). We consider the effective interaction between the pseudospins formed in two neighboring clusters in the a-b plane [panels (a)–(c)] and in the c direction of the crystal [panel (d)]. In cases (a) and (b) the two molecules are related by inversion symmetry whereas in (c) they are related by $C_2^{(z)}$ symmetry. In (d) the two molecules are related by translational symmetry. We take $U = 10t_c$ and the intracluster Heisenberg exchange $J_F = 0$ (Hubbard model) except in case (b) for which $J_F = -0.2t_c$. Anisotropic pseudospin exchange interactions arise when inversion symmetry is broken [cases (c) and (d)] and in the presence of inversion symmetry when $J_F \neq 0$ [case (b)]. We take $t = t_z = 0.785t_c$ in all plots.

Interestingly, for $J_F \neq 0$ all three diagonal exchange couplings of the tensor become different: $J^{ab}_{zz} > J^{ab}_{yy} > J^{ab}_{xx}$ [Fig. 4(b)]. Hence, for $J_F \neq 0$ magnetic anisotropies between the pseudospins are enhanced even in the presence of inversion symmetry. The two molecule problem has C_{2h} symmetry once SOC is included. Since all irreducible representations of C_{2h} are one dimensional we should then expect anisotropic couplings between the complexes that lift completely the energy level degeneracies present in the isolated trimers (Fig. 2). However, these level degeneracies persist in the spectrum of a pair of molecules for $J_F = 0$ since the in-plane exchanges ($J^{ab}_{xx} = J^{ab}_{yy}$) are equal in this case. Thus, lowering the symmetry of the Coulomb interaction (e.g., $J_F \neq 0$) can significantly increase the exchange anisotropy, as in models of transition metal oxides [7,34].

Finally we mention that the trigonal splitting D is only weakly affected by J_F [compare Figs. 4(a) and 4(b)]. The off-diagonal exchange $J^{ab}_{\alpha\beta}$ and non-pseudospin-conserving $K_{\alpha\beta}$ terms are nonzero, but remain small ($\sim 10^{-4}t_c$), for the parameters explored in Fig. 4(b).

It is important to understand what happens in the absence of an inversion center relating neighboring complexes. A particularly interesting case is if the two molecules are related by a rotation of π about a z axis bisecting the two molecules ($C_2^{(z)}$ symmetric). In the absence of SOC the $C_2^{(z)}$ symmetric and inversion symmetric models are identical. But the pseudovectorial nature of angular momenta implies that for a pair of molecules, l and m, related by $C_2^{(z)}$ symmetry $\lambda_{m,xy} = -\lambda_{l,xy}$ and $\lambda_{m,z} = \lambda_{l,z}$. With these relations the canonical transformation again yields an effective pseudospin Hamiltonian given by Eq. (7); but in contrast to the inversion symmetric case we now have $\eta = (-1)^{l+1}$ and $J^{ab}_{\beta\alpha} = -J^{ab}_{\alpha\beta}$ for $\alpha \neq \beta$. Furthermore $J^{ab}_{xx} \approx J^{ab}_{zz} \neq J^{ab}_{yy}$, within this $C_2^{(z)}$ symmetric model, and $J^{ab}_{xy} = J^{ab}_{yz} = 0$. The latter equality is straightforward since the Hamiltonian is real when written in the orbital basis. Because the off-diagonal exchange is antisymmetric these terms are equivalent to a Dzyaloshinskii-Moriya interaction, $\mathbf{D}_{lm} \cdot \boldsymbol{\mathcal{S}}_l \times \boldsymbol{\mathcal{S}}_m$ [35,36], with $D^y_{lm} = J^{ab}_{zx}$ and $D^x_{lm} = D^z_{lm} = 0$.

Anisotropies are large in the $C_2^{(z)}$ model [Fig. 4(c)], with J^{ab}_{zz} even becoming ferromagnetic for sufficiently large SOC: $\lambda > 1.7t_c$. J^{ab}_{zx} can become as large as the diagonal $J^{ab}_{\alpha\alpha}$ exchange couplings. The non-pseudospin-conserving terms induced by SOC at $O(\lambda^2)$ are found to be small compared to the other contributions [$K_{\alpha\beta}/t_c \sim 10^{-4} - 10^{-3}$ for the parameters explored in Fig. 4(c)]. The trigonal splitting is again large, with $D \approx J^{ab}_{yy} > J^{ab}_{\alpha\alpha}$ (with $\alpha = x,z$), at moderate values of $\lambda \approx 0.45t_c$.

B. *Nearest neighbors in the c direction*

Perpendicular to the plane the molecules stack in a tubular pattern [Figs. 1 and 4(d) inset] with the two clusters related by translational symmetry (no inversion symmetry center). The canonical transformation yields the effective pseudospin model:

$$H_c^{\text{eff}} = D\sum_l \left(\mathcal{S}_l^z\right)^2 + \sum_{\langle lm\rangle\alpha\beta} J^c_{\alpha\beta}\mathcal{S}^\alpha_l\mathcal{S}^\beta_m + \sum_{\langle lm\rangle\alpha\beta} P_{\alpha\beta}\mathcal{S}^\alpha_l\mathcal{S}^\beta_l\mathcal{S}^\alpha_m\mathcal{S}^\beta_m, \quad (8)$$

where anisotropic biquadratic couplings, $P_{\alpha\beta} = P_{\beta\alpha}$, obey $P_{zz} = 2P_{zx} = 2P_{zy}$ and $P_{xx} = P_{yy} = P_{xy} = 0$, see Appendix A 3. These relations are also confirmed numerically. The dependence of the nonzero couplings on λ is shown in Fig. 4(d) where $t = 0.785t_c$ is used for a clear comparison with the dumbbell arrangement. For $J_F = 0$ the off-diagonal couplings $J^c_{\alpha\beta} = 0$ for $\alpha \neq \beta$, whereas the diagonal terms behave as $J^c_{xx} = J^c_{yy} > J^c_{zz}$. Note that the isotropic version of model (8), i.e., $J^c_{\alpha\beta} = J^c\delta_{\alpha\beta}, P_{\alpha\beta} = P\delta_{\alpha\beta}$ and $D = 0$ is just the bilinear-biquadratic model: $H = J^c\mathbf{S}_l \cdot \mathbf{S}_m + P(\mathbf{S}_l \cdot \mathbf{S}_m)^2$, which becomes the Affleck-Kennedy-Lieb-Tasaki (AKLT) model for $P/J^c = 1/3$, which has the valence bond solid ground state and is in the Haldane phase [37].

The in-plane isotropy of the interlayer exchange ($J^c_{xx} = J^c_{yy}$, *etc.*) arises from the trigonal symmetry of the molecular packing (tube), in contrast to the symmetry of the in-plane packing (dumbbell) motif which allows $J^{ab}_{xx} \neq J^{ab}_{yy}$.

C. Beyond the low-energy effective models

A simple measure of the importance of charge fluctuations can be constructed from the comparison of the effective Hamiltonian with the exact solution of the two molecule (six site) problem. For instance, by comparing the exchange couplings obtained from our analysis with the exact energy gap δE, between the highest energy state included in our effective Hamiltonian and the lowest energy state not included in it, cf. Fig 3. For the dumbbell, case (A), with $\lambda = t_c$ and $U = 10t_c$ we find that $J^{ab} \approx 0.042 \ll \delta E = 0.6$, suggesting that in-plane charge fluctuations are small and localized spin moments are present. For the tube, case (B), $J^c \approx 0.3 > \delta E = 0.1$ for $U = 10t_c$ and $\lambda = t_c$, but $J^c \approx 0.15 < \delta E = 0.37$ for $U = 20t_c$ and $\lambda = t_c$. Thus, charge fluctuations in the c direction are clearly more important.

The difference between the tube and dumbbell are consistent with earlier studies of Hubbard chains on the necklace [23,24] and three-legged ladders [25] with no SOC. In these studies, it was found that the ground state of the model is a Haldane insulator down to very low U in contrast to naive expectations, since a Mott insulating state is not possible away from half filling. Hence, a Haldane insulator is robust against charge fluctuations which effectively suppresses the localized spin moments in the trimers below $S = 1$. This suppression is found to be stronger in three-legged ladders than in the necklace lattice [compare Fig. 1(a) in Ref. [25] with Fig. 3(b) in Ref. [23]].

The analytical results of our canonical transformation (Appendix A) provide key insight into the difference between the dumbbell and tube geometries. We note that the perturbative expressions for $J^c_{\alpha\alpha}$ for tubes, Eqs. (A3a)–(A3b), contains contributions of $O(t_z^2/t_c)$ not present in the dumbbell arrangement, Eqs. (A1b)–(A1d). This is because clusters in the tube arrangement can exchange particles through virtual processes without the energy cost of U, since the three vertices are connected by t_z in contrast to the dumbbell. As $t_z/t_c \simeq 0.68$ in $Mo_3S_7(dmit)_3$ (cf. Table I) one should worry whether fourth order processes, $O(t_z^4/t_c^3)$, only present in the tube arrangement, could lead to next-nearest-neighbor interactions which are comparable with the nearest-neighbor interactions of $O(t_z^2/t_c)$. However, the actual expansion parameter is $t_z/3t_c$ (not t_z/t_c). This factor of three is essentially the probability of an electron in a given molecular orbital being found on any particular site, i.e., it is the square of the prefactor $1/\sqrt{3}$ in Eq. (2). Therefore, fourth order terms, $\sim t_z^4/81t_c^3$, contain a prefactor nine times smaller than second order processes, $\sim t_z^2/9t_c$. Hence, for $Mo_3S_7(dmit)_3$ we estimate that the next-nearest-neighbor exchange coupling is about 20 times smaller than the nearest neighbor exchange coupling along the tube. These estimates imply a good convergence of the perturbation theory used providing further validity of our low energy effective spin exchange model obtained along the c direction of $Mo_3S_7(dmit)_3$, Eq. (8).

IV. QUASI-ONE-DIMENSIONAL PSEUDOSPIN-ONE MODEL FOR TRINUCLEAR COMPLEXES

Comparing the magnitude of the diagonal exchange couplings in the a-b plane, $J^{ab}_{\alpha\alpha}$ [Figs. 4(a)–4(c)], with the

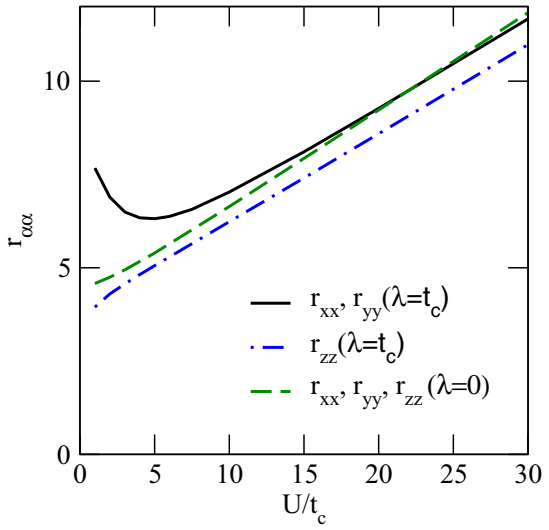

FIG. 5. Effective one-dimensionality arising from electron correlations in trinuclear complexes. As the on-site Coulomb repulsion (U) increases spatial anisotropy of the exchange coupling, $r_{\alpha\alpha} = J^c_{\alpha\alpha}/J^{ab}_{\alpha\alpha}$, is enhanced driving the crystal to a quasi-one-dimensional system. We have taken $t = t_z = 0.785t_c$.

pseudospin exchange couplings in the c direction, $J^c_{\alpha\beta}$ [Fig. 4(d)], one finds significant spatial anisotropy: $r_{\alpha\alpha} = J^c_{\alpha\alpha}/J^{ab}_{\alpha\alpha} \gg 1$. Furthermore, $r_{\alpha\alpha}$ increases rapidly with U, see Fig. 5. Indeed $J^{ab}_{\alpha\alpha} \to 0$ for all α as $U \to \infty$ independent of the other parameters in the Hamiltonian [see Eqs. (A1b)–(A1d)]. In contrast all $J^c_{\alpha\alpha}$ remain finite [see Eqs. (A3a)–(A3b)] as $U \to \infty$ in the absence of fine tuning of λ_{xy}, λ_z, and t_c.

This is because clusters along the c direction can exchange virtual particles while paying no energy U cost in contrast to clusters in the a-b plane which are connected through one hopping amplitude t. This difference leads directly to an emergent quasi-one-dimensional system for intermediate or large U [38]. Thus, even though the underlying electronic structure is almost isotropic, strong electronic correlations result in a quasi-one-dimensional spin model. Hence, in the strong coupling limit, the effective model for trinuclear complexes consists of weakly coupled antiferromagnetic pseudospin-one chains described by model (8).

V. CONCLUSIONS AND OUTLOOK

Our work shows how antiferromagnetic pseudospin-one chains arise along the c direction in crystals of trinuclear complexes such as $Mo_3S_7(dmit)_3$ and its selenated analogs. With no SOC, these chains can be modeled through an isotropic $S = 1$ Heisenberg model whose ground state is in the Haldane phase [23,25]. An important question is whether the Haldane phase is stable to the weak exchange coupling between neighboring chains arranged in the hexagonal geometry. Previous numerical work [39] has shown how the Haldane phase is unstable to the interchain exchange coupling when $r_{\alpha\alpha} = J^c_{\alpha\alpha}/J^{ab}_{\alpha\alpha} > 3$ in the hexagonal geometry of $Mo_3S_7(dmit)_3$ crystals. Since, $r_{\alpha\alpha} \gtrsim 5$ for all α, for even moderate U, we expect the Haldane phase to be the ground state of the crystal for weak SOC.

Turning on SOC introduces a trigonal splitting D as well as anisotropic spin exchange couplings. Thus, increasing SOC can drive the crystal from a topological Haldane phase to a trivial 'D phase' consisting of the tensor product of $j = 0$ states on each molecule. Hence, a quantum phase transition [40] may be induced in the family of materials based on $Mo_3S_7(dmit)_3$ crystals by substituting, say, Mo → W [20] or S → Se [14], which effectively increases the SOC. Intriguingly, although several selenated analogs of $Mo_3S_7(dmit)_3$ have been synthesized [17], little is known about their magnetic properties.

ACKNOWLEDGMENTS

J.M. acknowledges financial support from: (MAT2015-66128-R) MINECO/FEDER, UE. Work at the University of Queensland was supported by the Australian Research Council (FT130100161, DP130100757, and DP160100060).

APPENDIX: EFFECTIVE EXCHANGE COUPLINGS FROM PERTURBATION THEORY

Here we give analytic expressions for the parameters in Eqs. (7) and (8) to first order in $1/U$ and second order in H_{SO} and H_{kin} for the different configurations of the trimers discussed in the paper.

1. Complexes related by inversion symmetry

For the nearest neighbor complexes in the a-b plane related by inversion symmetry, the parameters in the effective Hamiltonian (7) to leading order in $J_c = J_F + 4t_c^2/U$ and second order in H_{SO} and H_{kin}, are:

$$J^{ab}_{\alpha\beta} = J^{ab}_{\beta\alpha}, \tag{A1a}$$

$$J^{ab}_{xx} = \frac{4t_g^2}{9U}\left[1 - \frac{1}{48}\left(\frac{\lambda_z}{t_c}\right)^2\right] + \frac{2t_g^2}{81}\left(\frac{4}{U} + \frac{J_F}{t_c^2}\right)\left[1 + \frac{5}{144}\left(\frac{\lambda_z}{t_c}\right)^2 - \frac{1}{2}\left(\frac{\lambda_{xy}}{t_c^2}\right)^2\right], \tag{A1b}$$

$$J^{ab}_{yy} = \frac{4t_g^2}{9U}\left[1 - \frac{1}{48}\left(\frac{\lambda_z}{t_c}\right)^2\right] + \frac{2t_g^2}{81}\left(\frac{4}{U} + \frac{J_F}{t_c^2}\right)\left[1 + \frac{5}{144}\left(\frac{\lambda_z}{t_c}\right)^2 - \frac{1}{3}\left(\frac{\lambda_{xy}}{t_c^2}\right)^2\right], \tag{A1c}$$

$$J_{zz}^{ab} = \frac{4t_g^2}{9U} + \frac{2t_g^2}{81}\left(\frac{4}{U} + \frac{J_F}{t_c^2}\right)\left[1 + \frac{1}{12}\left(\frac{\lambda_z}{t_c}\right)^2 - \frac{7}{12}\left(\frac{\lambda_{xy}}{t_c^2}\right)^2\right], \tag{A1d}$$

$$J_{xz}^{ab} = \frac{1}{\sqrt{2}}\frac{t_g^2}{486}\left(\frac{1}{U} + \frac{J_F}{4t_c^2}\right)\frac{\lambda_{xy}\lambda_z}{t_c^2}, \tag{A1e}$$

$$J_{yz}^{ab} = 0, \tag{A1f}$$

$$J_{xy}^{ab} = 0, \tag{A1g}$$

$$K_{z\pm} = \sqrt{2}\left[\frac{t_g^2}{81}\left(\frac{1}{6t_c^3} + \frac{11}{6t_c^2 U} + \frac{11J_F}{24t_c^4}\right)\right]\lambda_{xy}\lambda_z, \tag{A1h}$$

$$K_{\pm\pm} = \frac{t_g^2}{81}\left(\frac{2}{3U} + \frac{J_F}{6t_c^2}\right)\left(\frac{\lambda_{xy}}{t_c^2}\right)^2, \tag{A1i}$$

$$\begin{aligned} D = &\left[\frac{1}{6t_c} + \frac{1}{6U} + \frac{J_F}{24t_c^2}\right]\lambda_{xy}^2 - \left[\frac{1}{12t_c} - \frac{1}{6U} - \frac{J_F}{24t_c^2}\right]\lambda_z^2 \\ &- \frac{t_g^2}{81}\left[\frac{5}{24t_c^3}\lambda_z^2 + \left(\frac{43}{72t_c^2 U} + \frac{43J_c}{288t_c^4}\right)\lambda_z^2 - \left(\frac{1}{3t_c^2 U} + \frac{J_F}{12t_c^4}\right)\lambda_{xy}^2\right]. \end{aligned} \tag{A1j}$$

2. Complexes related by $C_2^{(z)}$

For complexes related by a rotation by π about the z axis then λ_{xy} must have equal magnitudes but opposite signs on the two complexes. For nearest neighbor complexes in the a-b plane the effective Hamiltonian to leading order in $1/U$ and second order in $H_{\rm SO}$ and $H_{\rm kin}$ is again given by Eq. (7) of the main text. To leading order in $J_c = J_F + 4t_c^2/U$ and second order in $H_{\rm SO}$ and $H_{\rm kin}$ one finds that J_{yy}^{ab}, $K_{z\pm}$, $K_{\pm\pm}$, and D are given by Eqs. (A1c), (A1h), (A1i), and (A1j), respectively, but

$$J_{xx}^{ab} = \frac{4t_g^2}{9U}\left[1 - \frac{1}{48}\left(\frac{\lambda_z}{t_c}\right)^2 - \frac{4}{9}\left(\frac{\lambda_{xy}}{t_c}\right)^2\right] + \frac{2t_g^2}{81}\left(\frac{4}{U} + \frac{J_F}{t_c^2}\right)\left[1 + \frac{5}{144}\left(\frac{\lambda_z}{t_c}\right)^2 - \frac{5}{18}\left(\frac{\lambda_{xy}}{t_c^2}\right)^2\right], \tag{A2a}$$

$$J_{zz}^{ab} = \frac{4t_g^2}{9U}\left[1 - \frac{4}{9}\left(\frac{\lambda_{xy}}{t_c}\right)^2\right] + \frac{2t_g^2}{81}\left(\frac{4}{U} + \frac{J_F}{t_c^2}\right)\left[1 + \frac{1}{12}\left(\frac{\lambda_z}{t_c}\right)^2 - \frac{13}{36}\left(\frac{\lambda_{xy}}{t_c^2}\right)^2\right], \tag{A2b}$$

$$J_{xz}^{ab} = -J_{zx}^{ab} = \frac{1}{\sqrt{2}}\frac{2t_g^2}{81}\left\{\left(\frac{76}{3U} + \frac{J_F}{3t_c^2}\right)\frac{\lambda_{xy}}{t_c} + \left(\frac{155}{36U} + \frac{11J_F}{144t_c^2}\right)\frac{\lambda_{xy}\lambda_z}{t_c^2}\right\}. \tag{A2c}$$

3. Effective Hamiltonian along the chains

For complexes stacked along the c axis, related by translational symmetry, the low-energy effective Hamiltonian is given by Eq. (4) of the main text to leading order in $1/U$ and second order in $H_{\rm SO}$ and $H_{\rm kin}$. To leading order in $J_c = J_F + 4t_c^2/U$ and second order in $H_{\rm SO}$ and $H_{\rm kin}$

$$J_{xx}^{c} = J_{yy}^{c} = \frac{4t_z^2}{3U} + \frac{t_z^2}{9}\left\{\frac{2}{t_c}\left[1 + \frac{1}{18}\left(\frac{\lambda_z}{t_c}\right)^2 - \frac{5}{36}\left(\frac{\lambda_{xy}}{t_c}\right)^2\right] + \left(\frac{4}{U} + \frac{J_F}{t_c^2}\right)\left[1 + \frac{1}{6}\left(\frac{\lambda_z}{t_c}\right)^2 - \frac{29}{72}\left(\frac{\lambda_{xy}}{t_c}\right)^2\right]\right\}, \tag{A3a}$$

$$J_{zz}^{c} = \frac{4t_z^2}{3U} + \frac{t_z^2}{9}\left\{\frac{2}{t_c}\left[1 + \frac{1}{36}\left(\frac{\lambda_z}{t_c}\right)^2 - \frac{5}{36}\left(\frac{\lambda_{xy}}{t_c}\right)^2\right] + \left(\frac{4}{U} + \frac{J_F}{t_c^2}\right)\left[1 + \frac{1}{12}\left(\frac{\lambda_z}{t_c}\right)^2 - \frac{4}{9}\left(\frac{\lambda_{xy}}{t_c}\right)^2\right]\right\}, \tag{A3b}$$

$$P_{zz} = \frac{t_z^2}{9}\left[\frac{1}{2t_c} + \frac{3}{U} + \frac{3J_F}{4t_c^2}\right]\left(\frac{\lambda_z}{t_c}\right)^2, \tag{A3c}$$

$$D = \left[\frac{1}{6t_c} + \frac{1}{6U} + \frac{J_F}{24t_c^2}\right]\lambda_{xy}^2 - \left[\frac{1}{12t_c} - \frac{1}{6U} - \frac{J_F}{24t_c^2}\right]\lambda_z^2 - \frac{t_z^2}{81}\left\{\left[\frac{7}{2t_c} + \frac{43}{2U}\right]\left(\frac{\lambda_z}{t_c}\right)^2 - \left(\frac{3}{2U} + \frac{3J_F}{8t_c^2}\right)\left(\frac{\lambda_{xy}}{t_c}\right)^2\right\}. \tag{A3d}$$

[1] M. Z. Hasan and C. L. Kane, Rev. Mod. Phys. **82**, 3045 (2010).
[2] X.-L. Qi and S.-C. Zhang, Rev. Mod. Phys. **83**, 1057 (2011).
[3] D. Pesin and L. Balents, Nat. Phys. **6**, 376 (2010).
[4] W. Witczak-Krempa, G. Chen, Y. Baek Kim, and L. Balents, Ann. Rev. Cond. Mat. Phys. **5**, 57 (2014).
[5] M. Dzero, K. Sun, V. Galitski, and P. Coleman, Phys. Rev. Lett. **104**, 106408 (2010).
[6] G. Jackeli and G. Khaliullin, Phys. Rev. Lett. **102**, 017205 (2009).
[7] N. B. Perkins, Y. Sizyuk, and P. Wölfle, Phys. Rev. B **89**, 035143 (2014).
[8] Y. Sizyuk, C. Price, P. Wölfle, and N. B. Perkins, Phys. Rev. B **90**, 155126 (2014).
[9] J. G. Rau, E. K.-H. Lee, and H.-Y. Kee, Annu. Rev. Condens. Matter Phys. **7**, 195 (2016).
[10] A. Kitaev, Ann. Phys. **321**, 2 (2006).
[11] A. Banerjee, C. A. Bridges, J.-Q. Yan, A. A. Aczel, L. Li, M. B. Stone, G. E. Granroth, M. D. Lumsden, Y. Yiu, J. Knolle, S. Bhattacharjee, D. L. Kovrizhin, R. Moessner, D. A. Tennant, D. G. Mandrus, and S. E. Nagler, Nat. Mat. **15**, 733 (2016).
[12] K. Kanoda and R. Kato, Ann. Rev. Cond. Matt. Phys. **2**, 167 (2011).
[13] B. J. Powell and R. H. McKenzie, Rep. Prog. Phys. **74**, 056501 (2011).
[14] S. M. Winter, R. T. Oakley, A. E. Kovalev, and S. Hill, Phys. Rev. B **85**, 094430 (2012).
[15] B. J. Powell, Coord. Chem. Rev. **295**, 46 (2015).
[16] R. Llusar and C. Vicent, Coord. Chem. Rev. **254**, 1534 (2010).
[17] A. L. Gushchin, R. Llusar, C. Vicent, P. A. Abramov, and C. J. Gómez-García, Eur. J. Inorg. Chem. **2013**, 2615 (2013).
[18] R. Llusar, S. Uriel, C. Vicent, J. M. Clemente-Juan, E. Coronado, C. J. Gómez-García, B. Braida, and E. Canadell, J. Am. Chem. Soc. **126**, 12076 (2004).
[19] A. C. Jacko, C. Janani, K. Koepernik, and B. J. Powell, Phys. Rev. B **91**, 125140 (2015).
[20] A. L. Khosla, A. C. Jacko, J. Merino, and B. J. Powell, arXiv:1606.04605.
[21] J.-K. Bao, J.-Y. Liu, C.-W. Ma, Z.-H. Meng, Z.-T. Tang, Y.-L. Sun, H.-F. Zhai, H. Jiang, H. Bai, C.-M. Feng, Z.-A. Xu, and G.-H. Cao, Phys. Rev. X **5**, 011013 (2015).
[22] H. Zhong, X. Y. Feng, H. Chen, and J. Dai, Phys. Rev. Lett. **115**, 227001 (2015).
[23] C. Janani, J. Merino, I. P. McCulloch, and B. J. Powell, Phys. Rev. Lett. **113**, 267204 (2014).
[24] C. Janani, J. Merino, I. P. McCulloch, and B. J. Powell, Phys. Rev. B **90**, 035120 (2014).
[25] H. L. Nourse, I. P. McCulloch, C. Janani, and B. J. Powell, arXiv:1606.04297.
[26] P. Fazekas, *Lecture Notes on Electron Correlation and Magnetism* (World Scientific, Singapore, 2008), p. 63.
[27] B. J. Powell, Sci. Rep. **5**, 10815 (2015).
[28] J. Merino, B. J. Powell, and R. H. McKenzie, Phys. Rev. B **73**, 235107 (2006).
[29] From our calculations we estimate that residual terms are at most of $\mathcal{O}(10^{-4}t_c)$.
[30] A. F. Albuquerque, C. J. Hamer, and J. Oitmaa, Phys. Rev. B **79**, 054412 (2009).
[31] S. Hu, B. Normand, X. Wang, and L. Yu, Phys. Rev. B **84**, 220402(R) (2011).
[32] A. Langari, F. Pollmann, and M. Siahatgar, J. Phys. Cond. Matt. **25**, 406002 (2013).
[33] Y.-C. Tzeng and M.-F. Yang, Phys. Rev. A **77**, 012311 (2008).
[34] T. Yildirim, A. B. Harris, A. Aharony, and O. Entin-Wohlman, Phys. Rev. B **52**, 10239 (1995).
[35] I. Dzyaloshinski, J. Phys. Chem. Solids **4**, 241 (1958).
[36] T. Moriya, Phys. Rev. **120**, 91 (1960).
[37] I. Affleck, T. Kennedy, E. H. Lieb, and H. Tasaki, Phys. Rev. Lett. **59**, 799 (1987).
[38] Interference effects also lead to a quasi-one-dimensional band structure in $Mo_3S_7(dmit)_3$ [19] despite the similarity of t and t_z. However, these interference effects are of $\mathcal{O}(t^6)$ so they do not occur in the present $\mathcal{O}(t^2)$ analysis.
[39] K. Wierschem and P. Sengupta, JPS Conf. Proc. **3**, 012005 (2014).
[40] J.-S. Xia, A. Ozarowski, P. M. Spurgeon, A. G. Baldwin, J. L. Manson, and M. W. Meisel, arXiv:1409.5971.